

Decay of persistent spin helix due to the spin relaxation at boundaries

Valeriy A. Slipko,^{1,2} Anastasia A. Hayeva,² and Yuriy V. Pershin^{1,*}

¹*Department of Physics and Astronomy and USC Nanocenter, University of South Carolina, Columbia, South Carolina 29208, USA*

²*Department of Physics and Technology, V. N. Karazin Kharkov National University, Kharkov 61077, Ukraine*

(Received 8 November 2012; published 28 January 2013)

We study electron spin relaxation in one-dimensional structures of finite length in the presence of Bychkov-Rashba spin-orbit coupling and boundary spin relaxation. Using a spin kinetic equation approach, we formulate boundary conditions for the case of a partial spin polarization loss at the boundaries. These boundary conditions are used to derive corresponding boundary conditions for a spin drift-diffusion equation. The latter is solved analytically for the case of relaxation of a homogeneous spin polarization in one-dimensional finite-length structures. It is found that the spin relaxation consists of three stages (in some cases, two)—an initial D'yakonov-Perel' relaxation is followed by spin helix formation and its subsequent decay. Analytical expressions for the decay time are found. We support our analytical results by results of Monte Carlo simulations.

DOI: [10.1103/PhysRevB.87.035430](https://doi.org/10.1103/PhysRevB.87.035430)

PACS number(s): 72.15.Lh, 71.15.Pd, 71.70.Ej, 72.25.Dc

I. INTRODUCTION

Dynamics of electron spin polarization in semiconductor structures has attracted a lot of attention recently in the context of spintronics,^{1–3} which is playing a fundamental role in novel technological developments based on different effects in this scientific area. Moreover, the ability to understand and predict the dynamics of electron spins in semiconductors is also important for the area of two-terminal electronic devices with memory, so-called memristive devices.^{4–8} In some of them,^{4,6} the electron spin degree of freedom defines their internal state and, consequently, is responsible for their time-dependent memory response.

Currently, much attention is focused on one-dimensional (1D) systems with spin-orbit coupling since they demonstrate a variety of unexpected and useful properties.^{9–16} In particular, it has been shown by us recently^{14,15} that the electron spin relaxation in finite-length wires¹⁴ and certain two-dimensional (2D) channels¹⁵ is drastically different from that in infinite 1D or 2D systems: Instead of relaxing to zero, the homogeneous electron spin polarization relaxes into a persistent spin polarization structure known as the spin helix,^{17–20} a spin polarization configuration in which the direction of spin polarization density rotates along the wire (see Fig. 1). Moreover, system boundaries significantly modify the dynamics of spin relaxation in finite-size 2D systems,²¹ decreasing the spin relaxation rate.

In real experimental situations, the spin helix configuration cannot exist infinitely long. Here, we assume that the main decay mechanism is due to spin relaxation at system boundaries. Indeed, local strong random electric fields in the vicinity of boundaries result in a random spin-orbit interaction influencing the electron spin degree of freedom. It is thus important to develop a theory and model spin relaxation in constrained geometries taking into account the boundary spin relaxation and understand how the boundary spin relaxation changes the overall character of electron spin relaxation in the entire system.

In this paper, we use both spin kinetic¹⁵ and diffusion^{20,22–25} equations to investigate the dynamics of electron spin polarization in semiconductor wires of finite length. Specifically, we

consider the dynamics of spin relaxation in one-dimensional (1D) finite-length systems with a Bychkov-Rashba²⁶ spin-orbit interaction and boundary spin relaxation. Since it is easier to incorporate the boundary spin relaxation into the boundary conditions for spin kinetic equations,¹⁵ below we use the spin kinetic equation approach first. Next, based on boundary conditions for the spin kinetic equations, we derive boundary conditions for the spin diffusion equation, which is easier to solve. Finally, we obtain an exact solution for the problem of spin relaxation in a finite-length wire. Our analytical studies are complemented by semiclassical Monte Carlo simulations of spin dynamics,²⁷ giving additional insight into the problem.

II. MODEL AND BOUNDARY CONDITIONS

Let us consider electrons in a wire with a Bychkov-Rashba²⁶ spin-orbit interaction. It is assumed that between different scattering events, the electron Hamiltonian is given by

$$H = H_0 + H_R = \frac{\hat{p}^2}{2m} - \alpha\sigma_y\hat{p}, \quad (1)$$

where \hat{p} is the x component of the electron momentum operator, m is the effective electron's mass, σ_y is the Pauli matrix, and α is the spin-orbit coupling constant. One can show²⁸ that the quantum-mechanical evolution of a spin of an electron with a momentum \mathbf{p} can be reduced to a spin rotation with the angular velocity $\Omega = 2\alpha p/\hbar$ about the axis determined by the unit vector $\mathbf{n} = \mathbf{p} \times \mathbf{z}/p$. The scattering events such as, for example, due to phonons or impurities, randomize the electron trajectories and, correspondingly, the spin precession axis. This causes an average spin relaxation (the D'yakonov-Perel' spin relaxation mechanism^{29,30}).

A kinetic description of electron spin polarization in one-dimensional wires can be given¹⁵ in terms of vectors \mathbf{S}^+ and \mathbf{S}^- , which are the spin polarizations of electrons moving along the wire in the positive (with momentum $\mathbf{p} = m\mathbf{v}\mathbf{e}_x$) and negative ($\mathbf{p} = -m\mathbf{v}\mathbf{e}_x$) x directions with the average velocity $v = l/\tau$, where l is the mean free path and τ is the momentum relaxation time. The kinetic equation can be written as a system

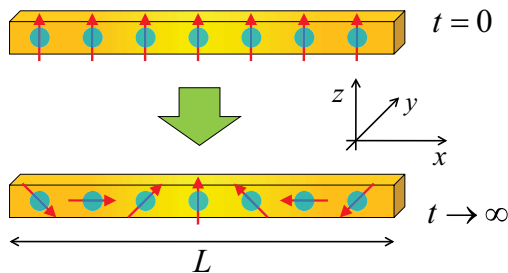


FIG. 1. (Color online) Transformation of homogeneous spin polarization into a persistent spin helix in a wire of length L with Bychkov-Rashba spin-orbit coupling *without* boundary spin relaxation (modified from Ref. 14).

of two vector equations,¹⁵

$$\left(\frac{\partial}{\partial t} + v\frac{\partial}{\partial x}\right)\mathbf{S}^+ = -\Omega\mathbf{e}_y \times \mathbf{S}^+ - \frac{1}{2\tau}(\mathbf{S}^+ - \mathbf{S}^-), \quad (2)$$

$$\left(\frac{\partial}{\partial t} - v\frac{\partial}{\partial x}\right)\mathbf{S}^- = \Omega\mathbf{e}_y \times \mathbf{S}^- - \frac{1}{2\tau}(\mathbf{S}^- - \mathbf{S}^+), \quad (3)$$

which take into account electron spin precessions [the first term on the right-hand side (rhs) of Eqs. (2) and (3)] induced by a Bychkov-Rashba²⁶ spin-orbit interaction [the second term on the rhs of Eq. (1)] and bulk scattering events [the second term on the rhs of Eqs. (2) and (3)]. Here, $p = mv$ is the average momentum, and \mathbf{e}_y is the unit vector in the y direction. Additionally, it is convenient to introduce the parameter $\eta = \Omega/v = 2\alpha m\hbar^{-1}$, which gives the spin precession angle per unit length. Note that the direction of spin precessions in Eqs. (2) and (3) is different for left- and right-moving electrons.

Equations (2) and (3) incorporate the well-known D'yakonov-Perel' spin relaxation mechanism.^{29,30} Indeed, trajectories of spin-polarized electrons are randomized by bulk scattering events described by the second term on the rhs of Eqs. (2) and (3). Correspondingly, the direction of spin rotation becomes fluctuating, which causes average spin relaxation (dephasing). The incomplete spin relaxation in finite-length wires¹⁴ can be explained by the existence of a maximum electron spin precession angle defined by the system size.

In this work, we study the dynamics of spin polarization in a wire of the length L , $-L/2 < x < L/2$, in the presence of spin relaxation at the boundaries $\Gamma = [x = \pm L/2]$. The boundary conditions, which take into account the relaxation of spin polarization in elastic scatterings of electrons from the boundaries, can be formulated as

$$[\mathbf{S}^- = \gamma\mathbf{S}^+]_{|x=L/2}, \quad (4)$$

$$[\mathbf{S}^+ = \gamma\mathbf{S}^-]_{|x=-L/2}, \quad (5)$$

where γ , $0 \leq \gamma \leq 1$, is a phenomenological dimensionless parameter characterizing the boundary relaxation rate. If $\gamma = 1$, then the spin polarization of scattered electrons is conserved (no boundary spin relaxation). The case $\gamma = 0$ corresponds to the total relaxation of spin polarization at the boundary, whereas for $0 < \gamma < 1$ we deal with a situation of a partial boundary relaxation.

Combining Eqs. (2) and (3) we obtain a single equation for the total spin polarization $\mathbf{S} = \mathbf{S}^+ + \mathbf{S}^-$,

$$\frac{\partial^2 \mathbf{S}}{\partial t^2} + \frac{1}{\tau} \frac{\partial \mathbf{S}}{\partial t} - v^2 \frac{\partial^2 \mathbf{S}}{\partial x^2} - 2\Omega v \mathbf{e}_y \times \frac{\partial \mathbf{S}}{\partial x} + \Omega^2 (\mathbf{S} - S_y \mathbf{e}_y) = 0, \quad (6)$$

where S_y is the y component of \mathbf{S} . What are the boundary conditions for \mathbf{S} ? These can be derived reformulating the boundary conditions given by Eqs. (4) and (5) in terms of the function \mathbf{S} only. Subtracting Eq. (3) from Eq. (2) we find

$$\frac{\partial}{\partial t}(\mathbf{S}^+ - \mathbf{S}^-) + v\frac{\partial \mathbf{S}}{\partial x} + \Omega\mathbf{e}_y \times \mathbf{S} + \frac{1}{\tau}(\mathbf{S}^+ - \mathbf{S}^-) = 0. \quad (7)$$

Now, let us consider, for example, the boundary $x = L/2$. From Eq. (4) we see that at $x = L/2$, $\mathbf{S}^+ = \mathbf{S}/(1 + \gamma)$, and $\mathbf{S}^- = \gamma\mathbf{S}/(1 + \gamma)$. Substituting these boundary values into Eq. (7) we obtain the corresponding boundary condition that can be generally formulated for both boundaries as

$$\left[v\frac{\partial \mathbf{S}}{\partial x} + \Omega\mathbf{e}_y \times \mathbf{S} \pm \frac{1 - \gamma}{1 + \gamma} \left(\frac{\partial \mathbf{S}}{\partial t} + \frac{\mathbf{S}}{\tau} \right) \right]_{|x=\pm L/2} = 0. \quad (8)$$

It is important to keep in mind that S_y is not coupled to any other component of spin polarization [see Eqs. (6) and (8)]. Consequently, we can safely take out S_y from our consideration selecting $S_y(x, t = 0) = 0$.

Introducing a complex polarization

$$S = S_x + iS_z, \quad (9)$$

it is straightforward to rewrite Eq. (6) and boundary conditions (8) in a more compact form

$$\frac{\partial^2 S}{\partial t^2} + \frac{1}{\tau} \frac{\partial S}{\partial t} - v^2 \left(\frac{\partial}{\partial x} - i\eta \right)^2 S = 0, \quad (10)$$

$$\left[\frac{\partial S}{\partial x} - i\eta S \pm \frac{1 - \gamma}{1 + \gamma} \left(\frac{1}{v} \frac{\partial S}{\partial t} + \frac{S}{v\tau} \right) \right]_{|x=\pm L/2} = 0. \quad (11)$$

The diffusion limit of Eqs. (10) and (11) is realized when $L \gg l$, $\eta l \ll 1$, and $t \gg \tau$. In this case we can neglect $\partial^2 S / \partial t^2$ compared to $\tau^{-1} \partial S / \partial t$ in Eq. (10) and $\partial S / \partial t$ compared to S / τ in Eq. (11), because all relevant spin relaxation times are much longer than the momentum relaxation time τ . As a result, we obtain

$$\frac{\partial S}{\partial t} = \frac{l^2}{\tau} \left(\frac{\partial}{\partial x} - i\eta \right)^2 S, \quad (12)$$

$$\left(\frac{\partial S}{\partial x} - i\eta S \pm \frac{1 - \gamma}{1 + \gamma} \frac{S}{l} \right)_{|x=\pm L/2} = 0. \quad (13)$$

The initial condition for Eq. (12) is

$$S(x, t = 0) = S_0(x). \quad (14)$$

We can exclude the rotations of the spin polarization vector [defined by Eq. (9)] that are still present in Eqs. (12) and (13) by introducing a complex field u via

$$u(x, t) = e^{-i\eta x} S(x, t). \quad (15)$$

Note that the rotation transformation (15) is a particular case of more general transformations that can be used to remove

spin precession.³¹ It can be shown¹⁴ that Eqs. (12) and (13) transform into the ordinary heat equation

$$\frac{\partial u}{\partial t} = D \frac{\partial^2 u}{\partial x^2}, \quad (16)$$

with the boundary condition

$$\left(\frac{\partial u}{\partial x} \pm \frac{1 - \gamma}{1 + \gamma} \frac{u}{l} \right) \Big|_{x=\pm L/2} = 0, \quad (17)$$

where $D = l^2/\tau$. Note that in the diffusion approximation y component of spin polarization S_y satisfies the same Eqs. (16) and (17).

III. RELAXATION OF HOMOGENEOUS POLARIZATION IN FINITE-LENGTH WIRES

We find the general solution of Eq. (16) with the boundary conditions (17) using the standard method of separation of variables. The straightforward application of this method leads to the following expression for the complex spin polarization:

$$S = e^{i\eta x} \sum_{n=1}^{+\infty} \left(a_n e^{-\frac{4\mu_n^2 D}{L^2} t} \sin \frac{2\mu_n x}{L} + b_n e^{-\frac{4\xi_n^2 D}{L^2} t} \cos \frac{2\xi_n x}{L} \right), \quad (18)$$

where μ_n and ξ_n are positive roots of

$$\tan \mu_n = -\kappa \mu_n \quad \text{and} \quad \cot \xi_n = \kappa \xi_n, \quad (19)$$

and $\kappa = 2(1 + \gamma)l/[(1 - \gamma)L]$.

Thinking about relaxation of an initial spin polarization profile, it is evident that an ‘‘overall’’ spin relaxation rate is determined by the smallest of the roots of Eqs. (19), which is the root ξ_1 satisfying the inequality $0 < \xi_1 < \pi/2$ (note that $\pi/2 < \mu_1 < \pi$). We can find explicit expressions for the spin relaxation time $\tau_r = L^2/(4D\xi_1^2)$ in the limiting cases of small and large κ . Specifically, when $\kappa \ll 1$ (the limit of strong boundary spin relaxation),

$$\xi_1 = \frac{\pi}{2}(1 - \kappa) \quad \text{and} \quad \tau_r = \frac{L^2 \tau}{\pi^2 l^2} (1 + 2\kappa). \quad (20)$$

In the opposite limit, when $\kappa \gg 1$ (the limit of weak boundary spin relaxation), we obtain

$$\xi_1 = \frac{6\kappa - 1}{6\kappa^{\frac{3}{2}}} \quad \text{and} \quad \tau_r = \frac{(1 + \gamma)[1 + (3\kappa)^{-1}]L\tau}{2(1 - \gamma)l}. \quad (21)$$

There are two additional time scales in the problem—the D’yakonov-Perel’ spin relaxation time, $\tau_{\text{DP}} = \tau/(l\eta)^2$, and the time of persistent spin helix formation in the absence of boundary spin scattering, τ_h . As these time scales are hidden in the set of relaxation times describing the dynamics of the general solution [Eq. (18)], we refer to our prior publication¹⁴ where the expression for τ_h is given, $\tau_h = L^2/(\pi^2 D)$. It is interesting that τ_h cannot exceed τ_r , namely, $\tau_r \geq \tau_h$. Consequently, when $\tau_r \gg \tau_h$, the spin dynamics can be considered as a three-stage process: An initial D’yakonov-Perel’ spin relaxation (i) is followed by spin helix formation (ii), which is followed by its decay (iii). Otherwise, when τ_r and τ_h are close, the decay stage significantly overlaps with the spin helix formation and thus stages (ii) and (iii) cannot be well separated.

In the case of three-stage dynamics, the spin helix amplitude (at the end of the second stage) is defined by the relation between τ_{DP} and τ_h times. In particular, if $\tau_h \gg \tau_{\text{DP}}$ (or, equivalently, $L\eta \gg \pi$), then the spin helix amplitude is much smaller than the amplitude of the initial spin polarization. In the opposite regime, when $\tau_h \lesssim \tau_{\text{DP}}$ (or $L\eta \lesssim \pi$), the spin helix amplitude is comparable to the initial one.

As an application of the above theory, let us consider a specific problem—the problem of relaxation of initially homogeneous spin polarization pointing in the z direction. In this case, the initial condition simply reads $S(x, 0) = iS_0$ [see Eq. (9)]. The coefficients a_n and b_n are obtained by substitution of this initial condition into Eq. (18), its multiplication by an appropriate sine or cosine function, and subsequent integration over x . This results in

$$\frac{a_n}{S_0} = \frac{4\mu_n \cos \mu_n [2 \sin(\eta L/2) + \eta L \kappa \cos(\eta L/2)]}{[(\eta L)^2 - 4\mu_n^2](1 + \kappa \cos^2 \mu_n)}, \quad (22)$$

$$\frac{b_n}{S_0} = i \frac{4\xi_n \sin \xi_n [2 \cos(\eta L/2) - \eta L \kappa \sin(\eta L/2)]}{[4\xi_n^2 - (\eta L)^2](1 + \kappa \sin^2 \xi_n)}. \quad (23)$$

Figure 2 demonstrates the dynamics of initially homogeneous spin polarization plotted using Eqs. (18), (22), and (23).

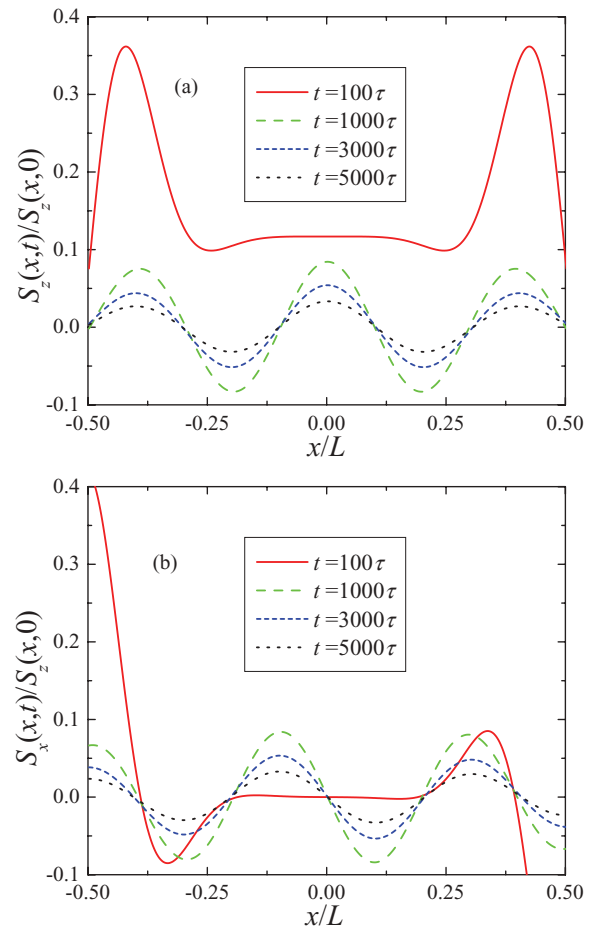


FIG. 2. (Color online) Relaxation of homogeneous spin polarization initially polarized in the z direction. (a) and (b) show the z and x components of spin polarization density at several moments of time. The wire length $L = 100l$, $\eta l = 0.1545$, $\gamma = 0.97$. These parameters result in $\kappa = 1.31$ and $\xi_1 = 0.78$.

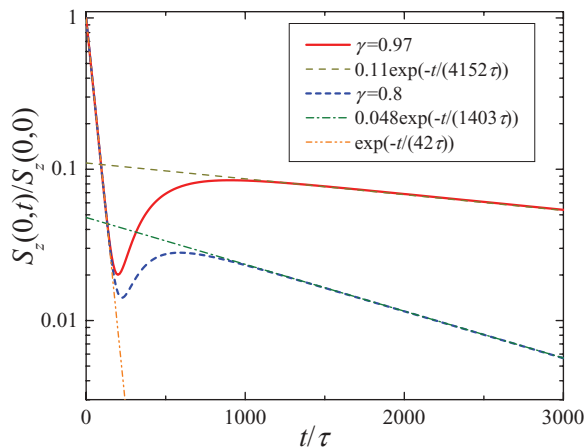


FIG. 3. (Color online) Temporal evolution of the spin polarization density S_z at the wire's center for the same parameter values as in Fig. 2. The fitting curves are obtained employing numerical values of τ_{DP} and τ_r calculated for these parameter values.

We emphasize that the initial relaxation at the center is of D'yakonov-Perel' type as, e.g., S_z and S_x in the central region (see $t = 100\tau$ curves) are flat. The spin helix configuration is clearly seen at $t \sim 1000\tau$. The subsequent slower evolution of spin polarization is caused by the boundary spin scattering. The boundary spin scattering results in smaller amplitudes of spin polarization oscillations closer to the ends and a larger amplitude at the wire's center.

Three stages of spin polarization dynamics, however, are better visualized plotting the magnitude of S_z at the wire's center as a function of time. Figure 3 shows $S_z(0,t)$ for two selected values of boundary spin scattering coefficient γ . Clearly, both curves contain two intervals of exponential relaxation that are seen on this logarithmic plot as straight lines. The initial interval of D'yakonov-Perel' spin relaxation ($0 < t \lesssim 200\tau$) is not influenced by the boundary spin relaxation. The latter, however, determines the character of spin relaxation at long times $750\tau \lesssim t$. The interval of spin helix formation ($200\tau \lesssim t \lesssim 750\tau$) is located between two regions of exponential evolution mentioned above.

In order to obtain additional insight on spin relaxation with boundary spin scattering, we have performed Monte Carlo simulations using an approach described in Refs. 32 and 27. This approach is based on a semiclassical description of electron space motion and a quantum-mechanical description of spin dynamics. All the main parts of the Monte Carlo simulation algorithm are described in Refs. 32 and 27 and will not be repeated here. The only different feature of the code is the boundary spin scattering mechanism implemented in the following way. When an electron scatters from a boundary, the direction of its spin is inverted with a probability $p = (1 - \gamma)/2$. It is not difficult to notice that this part of the algorithm is equivalent to the boundary conditions [Eqs. (4) and (5)] for the spin kinetic equation.

There is an excellent agreement between our analytical results and the numerical Monte Carlo simulations. For example, let us consider the dynamics of spin relaxation in a finite-length wire with boundary spin scattering when the spin precession angle per mean free path is relatively small.

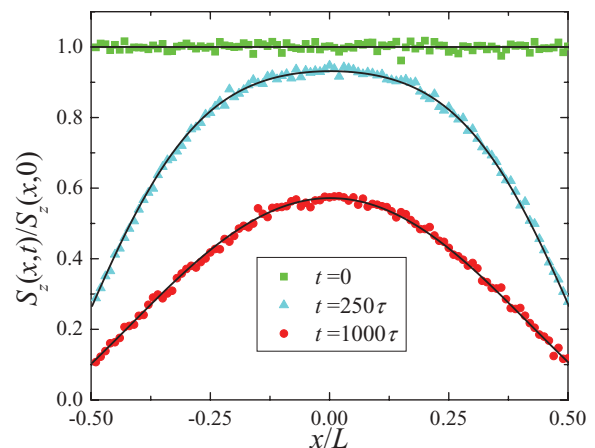


FIG. 4. (Color online) Comparison of the z component of spin polarization calculated analytically (straight lines) and numerically using Monte Carlo simulations (dots) for $L = 100l$, $\eta l = 0.01545$, $\gamma = 0.8$.

We also assume that at the initial moment of time $t = 0$, the spin polarization is homogeneous and points in the z direction. For this situation, Fig. 4 presents a comparison of S_z at different moments of time plotted using Eqs. (18), (22), and (23) (smooth curves) and Monte Carlo simulations (dots). We see that there is an excellent agreement between the analytical and numerical results.

Figure 4 shows a stronger distortion of the spin helix closer to the ends. This is a consequence of the diffusive dynamics that reduces the speed of spin polarization transfer along the wire. In the opposite ballistic regime of transport, when $l \gtrsim L$, we expect a faster formation of the spin helix (see Ref. 15) and its uniform decay. However, the ballistic regime is out of scope of this paper and is the subject for the future work.

IV. CONCLUSIONS

In conclusion, we have developed a theory of spin relaxation in wires accounting for boundary spin relaxation. For both spin kinetic and diffusion equations appropriate boundary conditions have been derived. Based on this theory, we predict the existence of three (in some cases, however, two) stages of spin dynamics consisting of an initial D'yakonov-Perel' relaxation followed by spin helix formation and its subsequent decay. Experimentally, parameters of boundary spin relaxation can be extracted from both the long-time spin helix decay rate and spin helix shape distortion. In addition to the spin relaxation in finite-length wires with Rashba spin-orbit coupling, our theory can also be applied to describe spin relaxation in certain 2D channels in the presence of both Rashba and Dresselhaus spin-orbit couplings of equal strength (see Ref. 15 for more details).

ACKNOWLEDGMENT

This work has been partially supported by the University of South Carolina ASPIRE Grant No. 13070-12-29502.

*pershin@physics.sc.edu

- ¹I. Zutic, J. Fabian, and S. Das Sarma, *Rev. Mod. Phys.* **76**, 323 (2004).
- ²S. Bandyopadhyay and M. Cahay, *Introduction to Spintronics* (CRC, Boca Raton, FL, 2008).
- ³M. Wu, J. Jiang, and M. Weng, *Phys. Rep.* **439**, 61 (2010).
- ⁴Y. V. Pershin and M. Di Ventra, *Phys. Rev. B* **78**, 113309 (2008).
- ⁵M. Di Ventra, Y. V. Pershin, and L. O. Chua, *Proc. IEEE* **97**, 1717 (2009).
- ⁶Y. V. Pershin and M. Di Ventra, *Adv. Phys.* **60**, 145 (2011).
- ⁷L. O. Chua, *IEEE Trans. Circuit Theory* **18**, 507 (1971).
- ⁸L. O. Chua and S. M. Kang, *Proc. IEEE* **64**, 209 (1976).
- ⁹Y. Kanai, R. Deacon, S. Takahashi, A. Oiwa, K. Yoshida, K. Shibata, K. Hirakawa, Y. Tokura, and S. Tarucha, *Nat. Nanotechnol.* **6**, 511 (2011).
- ¹⁰A. Bringer and T. Schäpers, *Phys. Rev. B* **83**, 115305 (2011).
- ¹¹S. Estévez Hernández, M. Akabori, K. Sladek, C. Volk, S. Alagha, H. Hardtdegen, M. G. Pala, N. Demarina, D. Grützmacher, and T. Schäpers, *Phys. Rev. B* **82**, 235303 (2010).
- ¹²J. A. Nesteroff, Y. V. Pershin, and V. Privman, *Phys. Rev. Lett.* **93**, 126601 (2004).
- ¹³C. Kloeffer, M. Trif, and D. Loss, *Phys. Rev. B* **84**, 195314 (2011).
- ¹⁴V. A. Slipko, I. Savran, and Y. V. Pershin, *Phys. Rev. B* **83**, 193302 (2011).
- ¹⁵V. A. Slipko and Y. V. Pershin, *Phys. Rev. B* **84**, 155306 (2011).
- ¹⁶M. M. Glazov and E. Y. Sherman, *Phys. Rev. Lett.* **107**, 156602 (2011).
- ¹⁷B. A. Bernevig, J. Orenstein, and S.-C. Zhang, *Phys. Rev. Lett.* **97**, 236601 (2006).
- ¹⁸C. P. Weber, J. Orenstein, B. A. Bernevig, S.-C. Zhang, J. Stephens, and D. D. Awschalom, *Phys. Rev. Lett.* **98**, 076604 (2007).
- ¹⁹J. D. Koralek, C. P. Weber, J. Orenstein, B. A. Bernevig, S.-C. Zhang, S. Mack, and D. D. Awschalom, *Nature (London)* **458**, 610 (2009).
- ²⁰Y. V. Pershin and V. A. Slipko, *Phys. Rev. B* **82**, 125325 (2010).
- ²¹V. A. Slipko and Y. V. Pershin, *Phys. Rev. B* **84**, 075331 (2011).
- ²²A. A. Burkov, A. S. Núñez, and A. H. MacDonald, *Phys. Rev. B* **70**, 155308 (2004).
- ²³E. G. Mishchenko, A. V. Shytov, and B. I. Halperin, *Phys. Rev. Lett.* **93**, 226602 (2004).
- ²⁴S. Saikin, *J. Phys.: Condens. Matter* **16**, 5071 (2004).
- ²⁵Y. V. Pershin, *Phys. E* **23**, 226 (2004).
- ²⁶Y. Bychkov and E. Rashba, *JETP Lett.* **39**, 78 (1984).
- ²⁷S. Saikin, Y. V. Pershin, and V. Privman, *Proc. Circuits Devices Syst.* **152**, 366 (2005).
- ²⁸Y. V. Pershin and V. A. Slipko, [arXiv:1007.0853v1](https://arxiv.org/abs/1007.0853v1); *Phys. Rev. B* **82**, 125325 (2010).
- ²⁹M. I. Dyakonov and V. I. Perel', *Sov. Phys. Solid State* **13**, 3023 (1972).
- ³⁰M. I. Dyakonov and V. Y. Kachorovskii, *Sov. Phys. Semicond.* **20**, 110 (1986).
- ³¹I. V. Tokatly and E. Y. Sherman, *Phys. Rev. B* **82**, 161305 (2010).
- ³²A. A. Kiselev and K. W. Kim, *Phys. Rev. B* **61**, 13115 (2000).